Establishment and Characterization of Novel Canine Organoids with Organ-Specific Physiological Similarity

Authors: Christopher Zdyrski[1,2]*, Vojtech Gabriel[1]*, Oscar Ospina[3], Hannah Wickham[1], Dipak K. Sahoo[4], Kimberly Dao[2], Leeann S. Aguilar Meza[1], Leila Bedos[4], Sydney Honold[1], Pablo Piñeyro[5], Jonathan P. Mochel[#1,2], Karin Allenspach[#1,2,4]

[1] SMART Pharmacology, Department of Biomedical Sciences, Iowa State University, Ames, IA, USA
[2] 3D Health Solutions Inc., Ames, IA, USA
[3] Department of Biostatistics and Bioinformatics, Moffitt Cancer Center, Tampa, FL, USA
[4] Department of Veterinary Clinical Sciences, Iowa State University, Ames, IA, USA
[5] Veterinary Diagnostic Laboratory, Iowa State University, Ames, IA, USA

*Authors contributed equally to the manuscript.
co-senior authors.

Corresponding authors: Christopher Zdyrski (czdyrski@iastate.edu); K. Allenspach (allek@iastate.edu) DVM, Ph.D.; Jonathan P. Mochel (jmochel@iastate.edu) DVM, Ph.D.

SUMMARY

Organoids are 3-dimensional (3D) stem cell-derived cell culture lines that offer a variety of technical advantages compared to traditional 2-dimensional (2D) cell cultures. Although murine models have proved useful in biomedical research, rodent models often fail to adequately mimic human physiology and disease progression, resulting in poor preclinical prediction of therapeutic drug efficacy and toxicity. With the advent of organoid technology, many of these challenges can be overcome. Previously, the use of canine organoids in drug testing and disease modeling was limited to organoids originating from the intestine, liver, kidney, and urinary bladder. Here, we report the cultivation, maintenance, and molecular characterization of three novel adult-stem cell-derived canine organoid cell lines, including the endometrium, lung, and pancreas, in addition to previously reported kidney, bladder, and liver organoids from two genetically related canines. Six tissues and organoid lines from each donor were characterized using bulk RNASeq, allowing for a unique, multi-organ comparison between these two individuals and identification of specific cell types such as glandular epithelial cells in endometrial organoids.

Keywords: canine; dog; organoids; reverse translational medicine; stem cell; endometrium; lung; pancreas; kidney; bladder; liver

INTRODUCTION

Numerous *in vitro* models are used as preclinical biological and pharmacological research tools (Hickman et al., 2014). The most prevalent *in vivo* models for biomedical research include *Drosophila melanogaster* and *Caenorhabditis elegans*, both of which are widely used for genetic research, *Danio rerio*, a model used primarily for mutagenesis screening, and numerous mammalian models for which advanced genetic tools are available (Kim et al., 2020b). Mouse models are extensively used in biomedical research due to their cost-effectiveness, fast-growing nature, and availability of genetic mutants (Kim et al., 2020b). Differences in diet, living environment, circadian rhythm, and the short lifespan are among the issues limiting the translational relevance of rodent models (Perlman, 2016). Although the murine model has proven effective in a variety of biological research areas, rodents frequently fail to adequately mimic human physiology and disease progression, hence compromising their predictive performance in preclinical pharmaceutical research (Gordon et al., 2009; Wang et al., 2018a). Approximately ninety percent of experimental drugs fail to make the transition from discovery to successful clinical trials (Mochel et al., 2018; van Norman, 2016; Shalev, 2006). Drug development is successful in about 5% of those ultimately approved, and average costs including post-approval R&D in the U.S. exceed $2 billion and it takes 10-15 years to reach clinical trials per drug (Brancato et al., 2020; DiMasi et al., 2016). The use of 3D organoids in the screening stage of drug discovery could drastically reduce the use of live animals for drug development (Mollaki, 2021). Ultimately, additional research is warranted to identify alternative *in vitro* models that can more accurately replicate human physiology and reduce animal use. Conventional pharmacology research involves using 2D cell culture and animal testing prior to human clinical trials (Brancato et al., 2020). The reverse translational paradigm, in which data from human clinical research might aid in the development of veterinary therapeutics and vice versa, is garnering a growing amount of interest (Schneider et al., 2018). Dogs share similar

lifestyles and diets with their owners due to the close relationship between dogs and humans, often including a sedentary lifestyle and an increased risk of developing obesity (Chandler et al., 2017). The longer lifespan of dogs over that of mice predisposes dogs to develop analogous chronic diseases to humans, including diabetes mellitus, inflammatory bowel disease, congestive heart failure, cancers, and cognitive dysfunction, among others (Adin and Gilor, 2017; Chandra et al., 2019; Knapp et al., 2020; Ozawa et al., 2019; Silva and Emter, 2020; Wang et al., 2018a). Therefore, dogs are typically used in preclinical drug safety assessments taking advantage of the available background scientific knowledge (Schaefer et al., 2016) stemming from veterinary medicine. While dogs excel as a model in many applications compared to rodents, they come with their own challenges in the form of expensive housing and ethical concerns about using live dogs in research. Dogs are recognized as companion animals in western countries, and there are ongoing worldwide initiatives to limit their use in research through the 3Rs (*Reduce*, *Replace*, *Refine*) principles (Hasiwa, 2011; Russell and Burch, 1959). A potential solution that provides more access to the canine model while decreasing reliance on live animal use lies in the organoid technology. Organoids are 3D self-organized, miniature, and simplified versions of organs *in vitro*. Adult stem cells can self-renew, differentiate into multiple cell types, and are genomically stable over multiple passages (Huch and Koo, 2015). Unlike traditional 2D cell lines, organoids grow in a 3D extracellular matrix, allowing for the recreation of more realistic tissue architecture and physiological responses (Hynds and Giangreco, 2013). Recently, donor-to-donor variability in human ileum- and colon-derived organoids has been investigated; however, more research is needed across other biomedical models, including dogs (Mohammadi et al., 2021). Furthermore, organoids can be used in both basic and applied biomedical research, including the study of genetic disorders, cancers, and infectious diseases (Kim et al., 2020b; Nantasanti et al., 2015; Usui et al., 2017; Zhou et al., 2018). Organoids can be a valuable tool for personalized medicine where patient-specific organoids can be grown and incubated with drug candidates to predict effectiveness prior to patient

treatment (Bartfeld and Clevers, 2017; Kaushik et al., 2018). Organoids may become useful for regenerative medicine; for example, hepatic organoids can be transplanted to a patient and transdifferentiated to various hepatocellular regional identities *in vivo* (Sampaziotis et al., 2021a). Organoid cell lines drastically reduce the number of animals needed for drug testing as they can be expanded indefinitely in culture and cryopreserved for future use. Organoid technology has made it possible to undertake pharmacological research and testing in a manner that is more responsible from an ethical standpoint, while also simplifying the process of genetic manipulation. While human organoids are a valuable research tool in the biomedical field, they come with limitations. Public concern plays a key role in tissue sampling from human patients (Lehmann et al., 2019). Ethical concerns for the use of human-derived organoids include chimeric research and genetic editing of organoids derived from patients (Munsie et al., 2017). Although a growing number of studies have characterized cell populations using transcriptomic data across human organs, there is a lack of similar studies in non-human models (Jones et al., 2022). Organoids still represent a relatively novel technology and lack formal standardization in isolation, maintenance, and downstream applications. We previously demonstrated the ability to culture canine intestinal organoids from healthy and diseased tissues and demonstrated the translational potential of these organoids for human medicine (Chandra et al., 2019). Our research group has been working to standardize the culture and maintenance of organoid cell lines to maximize the reproducibility of our findings across different experimental sites (Gabriel et al., 2022a). This investment into the standardization of protocols includes downstream applications such as the use of a permeable support system for canine organoids in drug testing and discovery (Gabriel et al., 2022b). Currently, there is a lack of canine organoid models compared to other major biomedical species to accurately depict and study various diseases, drugs, and biological phenomena.

This report describes the successful cultivation of three novel canine organoid lines of which none are published in a peer-reviewed journal, including the endometrium, lung, and pancreas,

in addition to previously described kidney (Chen et al., 2019), bladder (Elbadawy et al., 2022), and liver (Nantasanti et al., 2015) organoids from two related dogs. By comparing six tissue-specific organoid lines obtained from two genetically related donors, this study aims to acquire insight into gene expression in different organoids and their corresponding tissues. RNA sequencing, immunohistochemistry, and immunofluorescence were used to characterize the relationships between individual organoid cell lines and their parent tissue, further displaying potential applications in biomedical and translational medicine. In addition to the characterization of organoid lines, we compared related individuals across organs, further showcasing the use of 3D organoids for applications in personalized medicine.

RESULTS

Organoid Expansion

Organoid cell lines were successfully established from six organs, including the uterus, lung, pancreas, kidney, urinary bladder, and liver, three of which are novel, originating from two female canine individuals. All tissues were isolated on the same day, and organoids were cultivated simultaneously. Growth progression, passage number, and media supplementation information are reported in **Table S1.** Samples were passaged between two and four times before being harvested for characterization and inclusion into the biobank. A subset of the canine organoids displayed distinct morphological features characterized via light microscopy and hematoxylin & eosin (H&E) staining (**Figure 1**).

Morphological and histological characterization of canine organoid cell lines

Uterus

A subset of endometrial organoids formed a tubular structure appreciated on brightfield microscopy during culture (**Figure 1**). H&E staining suggested that the culture consists of endometrial epithelial cells and glandular epithelial cells (**Figure 1**). RNASeq data indicated that SRY-box transcription factor 17 (SOX17, family-wise error rate [FWER] = 1.63×10^{-9}) was upregulated in endometrium organoids (**Figure 2B**). This protein is expressed in the human endometrium, specifically in the luminal and glandular epithelium (Kinnear et al., 2019). SOX17 is important for endometrial glandular development and function in mice (Turco et al., 2017), and was also expressed in organoids derived from human menstrual flow, consistent with their function in endometrial gland development (Cindrova-Davies et al., 2021). Distal-less homeobox 6 (DLX6) was upregulated in both organoids (FWER = 1.56×10^{-5}) and tissues (FWER = 9.28×10^{-5}) (**Figures 2B and 2C**) in the dogs. DLX6 has been found to be upregulated in the human endometrium during the secretory phase of the cycle (Bellessort et al., 2016). Uroplakin Ib (UPK1B) was upregulated in endometrium organoids compared to uterus tissues (FWER = 4.50×10^{-4}) (**Figure 2A**). The top endometrium-specific genes for organoids included Actin gamma 1 (ACTG1), Prothymosin alpha (PTMA) and Thymosin beta 10 (TMSB10), whereas uterine tissues showed high expression of multiple ribosomal proteins (**Figure 2D**). Regarding endometrium-specific genes, organoids had 585 unique genes (**Figure 3A**), uterine tissues had 2,600 unique genes (**Figure 3B**), and 14,280 genes were expressed in both organoids and tissues (**Figure 3C**). For immunofluorescence (IF), Vimentin (VIM) was positive in both tissues and organoids (**Figure 4**).

Lung

The lung organoids displayed three distinct phenotypes with flowering differentiated organoids and bulbous organoids constituting most of the culture, while a small proportion had a morphology resembling alveolar structures (**Figure 1**). H&E staining suggests our culture consists of alveolar type-2 cells (AT2) and bronchial epithelial cells (**Figure 1**). The lung marker, NK2 homeobox 1 (NKX2-1) (Dost et al., 2020), was upregulated in organoids (FWER = 4.78×10^{-6}) (**Figure 2B**), while Surfactant Protein B (SFTPB) and Surfactant Protein C (SFTPC) gene expression were detected and specific to both lung tissues and organoids (**Figure 2D**). Upregulated genes in organoids compared to tissues included Pyroglutamylated RFamide peptide (QRFP) and Peptidoglycan recognition protein 1 (PGLYRP1). For lung-specific genes, organoids had 656 unique genes (**Figure 3A**), tissues had 1,250 unique genes (**Figure 3B**), and 14,283 genes were expressed in both organoids and tissues (**Figure 3C**). IF staining clearly identified alveolar type-1 cells (AT1) for Claudin 18 (CLDN18) in lung tissue, surprisingly organoids did express this marker (**Figure 4**).

Pancreas

The pancreatic organoids displayed two phenotypes, one resembling spheroids and another of a flowering organoid (**Figure 1**). H&E staining suggested that the culture mainly consisted of cells derived from intercalated ducts, with a few cells potentially differentiating into endocrine cells (**Figure 1**). Genes that were found to be upregulated in organoids compared to tissue included Dual oxidase 2 (DUOX2, FWER = 1.62×10^{-2}), Pyroglutamylated RFamide peptide (QRFP, FWER = 2.29×10^{-3}), Cadherin 17 (CDH17, FWER = 1.15×10^{-3}), and Early growth response 1 (EGR1, FWER = 2.97×10^{-3}) (**Figure 2A**). Noteworthy is that Somatostatin (SST, FWER = 4.39×10^{-3}) was suppressed in organoids suggesting our culture does not contain a significant number of delta cells (**Figure 2A**). Maltase-glucoamylase 2 (MGAM2, FWER = 3.23×10^{-3}) and NK6 homeobox 1 (NKX6-1, FWER = 1.44×10^{-4}) were also upregulated in organoids

(**Figure 2B**). NKX6-1 expression is a marker of multipotent pancreatic progenitors, which can differentiate into ductal, acinar, and endocrine cells (Wiedenmann et al., 2021). Upregulated genes in pancreas tissues included Insulin (INS, FWER = 3.04×10^{-4}), Glucagon (GCG, FWER = 1.33×10^{-3}), and multiple markers indicative of pancreatic acinar cells (**Figure 2C**). One of the most highly expressed pancreas-specific genes in the organoids included cytokeratin 7 (KRT7), indicating that most of the cells in the organoids are of epithelial origin and represent pancreatic ductal cells (Wiedenmann et al., 2021). Regarding pancreas-specific genes, organoids had 382 unique genes (**Figure 3A**), tissues had 259 unique genes (**Figure 3B**), and 13,872 genes were expressed in both organoids and tissues (**Figure 3C**). IF staining on pancreatic tissues identified insulin and glucagon in the islets (**Figure 4**); however, the organoids were not producing insulin nor glucagon.

Kidney

The kidney organoids displayed two distinct phenotypes, one resembling an organoid mass and the other resembling tubular structures (**Figure 1**). H&E staining identified multiple organoids containing structures resembling the glomerulus and Bowman's capsules as well as collecting ducts (**Figure 1**). No differentially expressed (DE) genes were identified between kidney organoids and tissues. SIM bHLH transcription factor 1 (SIM1) was upregulated in organoids (FWER = 2.66×10^{-2}) (**Figure 2B**) as well as tissues, (FWER = 3.66×10^{-4}) (**Figure 2C**) while POU class 3 homeobox 3 (POU3F3, FWER = 7.93×10^{-5}) was enriched in kidney organoids (**Figure 2B**) and is a distal tubular marker (Subramanian et al., 2019). Cathepsin B (CTSB) was one of the top ten kidney-specific markers expressed in both organoids and tissues (**Figure 2D**). Kidney-derived organoids had 1,277 unique genes (**Figure 3A**), and tissue had 2,512 unique genes (**Figure 3B**), with 14,735 genes expressed both in organoids and tissues (**Figure 3C**). Renal structures were characterized by IF in tissues and organoids. Within the tissue samples, distal tubular cells were identified by staining of Transmembrane Protein 52B (TMEM52B),

proximal tubules by Solute Carrier Family 5 Member 2 (SLC5A2) staining, and parietal epithelial cells were identified using Platelet Endothelial Cell Adhesion Molecule 1 (PECAM1) (**Figure 4**). Within the organoids, only TMEM52B stained positively by IF, clearly identifying distal tubular cells in the organoids (**Figure 4**).

Urinary Bladder

Bladder organoids displayed a single phenotype constituting round organoids without a visible lumen or internal chamber typical of spheroids of other tissues like intestine (**Figure 1**) (Chandra et al., 2019; Gabriel et al., 2022a). H&E staining showed the organoids present morphological features consistent with transitional epithelium (**Figure 1**). Desmoglein 3 (DSG3, FWER = 2.28×10^{-3}), which is a basal cell marker (Elbadawy et al., 2019), and Loricrin cornified envelope precursor protein (LORICRIN, FWER = 1.38×10^{-2}), an intermediate cell marker (Lin et al., 2013), were upregulated in organoids compared to tissues (**Figure 2A**). Uroplakin (UPK) proteins are specific to urothelial cells (Lu et al., 2022), and both Uroplakin 2 (UPK2, FWER = 1.70×10^{-2}) and Uroplakin 3A (UPK3A, FWER = 4.74×10^{-3}) were upregulated in organoids (**Figure 2B**). UPK3A is an umbrella cell marker, while Keratin 5 (KRT5) is indicative of basal cells and was bladder-specific and upregulated in the canine bladder organoids (Elbadawy et al., 2022; Kim et al., 2020a). The bladder-specific markers PFN1 and EIF4A1 were expressed in both organoids and tissues. Regarding bladder-specific genes, organoids had 797 unique genes (**Figure 3A**), tissues had 670 unique genes (**Figure 3B**), and 14,071 genes were expressed in both organoids and tissues (**Figure 3C**). The presence of umbrella cells and basal cells was confirmed by positive IF staining with Uroplakin Ia (UPK1A) and Cytokeratin 5 (CK5) (**Figure 4**) in tissues. UPK1A expression was present in the "pores" of umbrella cells, while expression of CK5 was positive and limited to the outside of the bladder organoids (**Figure 4**).

Liver

Liver organoids morphologically resembled the pancreatic organoids, with one phenotype resembling spheroids and another of a more flowering organoid. Cellular morphology observed under H&E evaluation suggest that most of the cells were differentiated cholangiocytes (**Figure 1**). Trefoil factor 1 (TFF1, FWER = 1.80×10^{-2}), Mucin 5B (MUC5B, FWER = 4.18×10^{-2}), and Tripartite Motif Containing 71 (TRIM71, FWER = 3.76×10^{-2}) were all upregulated in liver organoids compared to liver tissue (**Figure 2A**). TFF1 encodes a protein critical in the regeneration of the liver after injury by promoting biliary lineage differentiation and inhibiting hepatic lineage (Hayashi et al., 2018). Single-cell RNA sequencing of the human liver described a transcriptional profile of a cell population within cholangiocytes where the DE genes included TFF1 and MUC5B (MacParland et al., 2018). TRIM71 was also upregulated in organoids (FWER = 3.21×10^{-3}) (**Figure 2B**) and has previously been hypothesized to be involved in promoting rapid self-renewal in undifferentiated mouse embryonic stem cells (Chang et al., 2012). Liver-specific organoid markers included multiple heterogeneous nuclear ribonucleoproteins (**Figure 2D**). Albumin (ALB) was the most highly expressed liver-specific gene in tissue due to the large percentage of hepatocytes (**Figure 2D**). Regarding liver-specific genes, organoids had 2,003 unique genes (**Figure 3A**), tissues had 704 unique genes (**Figure 3B**), and 13,480 genes were expressed in both organoids and tissues (**Figure 3C**). Using IF, hepatocytes stained positively for Hydroxyacid Oxidase 1 (HAO1) (**Figure 4**) (Kampf et al., 2014). As expected, tissues showed high expression of HAO1 as hepatocytes constitute the major cell type in liver tissue while organoids were negative, suggesting they mainly consist of cholangiocytes.

DISCUSSION

Canine organoids as biomedical models

Canines can represent a superior model to the mouse for translational research applications, particularly because of their propensity to develop analogous chronic diseases to humans and share similar lifestyles; however, using canines for translational research does come with obstacles. Their use in research can be ethically questionable and resource-intensive. Organoids can overcome some of these challenges and could represent an excellent alternative to expand the biomedical applications of the canine model (**Figure 5C**). Developing novel canine organoid models will accelerate research efforts toward advanced veterinary therapeutics as well as for preclinical drug screening in human medicine. Furthermore, advances in organoid technology are being made in areas including personalized drug testing using patient-derived organoid cultures (Huch and Koo, 2015; Mullenders et al., 2019; Sampaziotis et al., 2021b).

Typically, studies report the cultivation of one tissue-specific organoid cell line, while others combine organoid lines from multiple individuals to make conclusions. By combining unrelated donors' information, one neglects donor-to-donor variability, thus ignoring relevant differences in biological information. We set out to expand the biomedical applications of the dog model while decreasing animal use through the development of novel canine organoid lines and the characterization of gene expression across tissues. Many laboratories utilize tissue-specific protocols and media supplemented with various growth factors to expand their organoids which can be costly and laborious (Kaushik et al., 2018; Tortorella et al., 2022). In the current study, all described cultures were grown under the same conditions using the same organoid expansion media (*Complete media with growth factors with ROCK inhibitor and GSK3β - CMGF+ R/G*) and differentiation media (*Complete media with growth factors - CMGF+*). Additionally, many protocols emphasize tissue removal to create a suspension of stem cells during organoid

isolations. Here, we show that the inclusion of tissue pieces during the initial growth can benefit the canine organoid expansion. This phenomenon may be due to intercellular signaling from the stem cells still attached to damaged tissue, resulting in the release of damage-associated signals, increasing the initial growth of the stem cells, or potentially due to the availability of the extracellular matrix from the tissue at the beginning of the culture.

We report the cultivation, characterization, and comparison of six organoid lines (endometrium, lung, pancreas, kidney, bladder, and liver), three of them novel, derived from the same animal, from two genetically related canine donors. This allows for a biological replicate as the donors are of the same litter, sex, and age. Additionally, the isolation, cultivation, and media composition were identical for the six organoid cell lines, eliminating the need for tissue-specific growth factors. To the best of the authors' knowledge, the data in this study, therefore, constitutes the most comprehensive comparison of tissue-specific expression in canine organoids available to date. These newly available canine organoids could be applied for rapid translational applications, such as the identification of new therapeutics, the study of genetic editing, and the development of better disease models. Due to the nature of the samples being derived from the same donors, these lines have the potential to be used in downstream experiments including organ-on-a-chip (Dongeun et al., 2010) and assembloid cultures (Birey et al., 2017).

Insights into organ-specific genes

Identification of DE genes between tissues and organoids (**Figure 2A**) assisted in the determination of the major cell populations present and absent in the organoid cell lines. Genes expressed were identified for each tissue type (**Figure 3C**) to emphasize the similarity of expression patterns of the organoid models compared with their tissue of origin. A comparison of mRNA expression across tissues and organoids can be seen in **Figure 3.** Between 78% and 82% (**Figure 3C**) of all expressed genes overlapped for each organ between tissues and

organoids. Noteworthy is that the pancreas and liver both had a larger number of expressed genes unique to organoids compared to genes solely expressed in tissue than any of the other organoid cultures.

Multidimensional scaling plots (**Figure 3D and 3E**) displayed the clustering of samples, further highlighting similar expression patterns seen across the epithelial organoids and their tissues of origin. Intra-organoid and intra-tissue comparisons identified upregulated genes (**Figure 2B and 2C**) and the ten most highly expressed tissue-specific genes (**Figure 2D**). The expression of unique and overlapping genes were further compared for each sample type (**Figure 3A and 3B**). Gene pathway analysis was performed identifying shared and distinct characteristics of each organ for both organoids and tissues (**Figure 5B**). The details of the enriched pathways for organoids and tissues are listed in **Figure 5D and 5E**. The following biological pathways were the most notable from the intra-organoid specific genes (**Figure 5D**); bladder – tissue development, endometrium – tissue development, kidney – multicellular organismal process, liver – cell cycle process, lung – localization, pancreas – regulation of multicellular organismal process. Intra-tissue specific genes had the following relevant biological pathways (**Figure 5E**); bladder – cell activation, uterus – regulation of nucleobase-containing compound metabolic process, kidney – transmembrane transport, liver – small molecule metabolic process, lung – cilium movement, pancreas - insulin secretion. This preliminary characterization will assist in determining potential applications for these novel canine organoid models for research applications.

Organoid characterization and biomedical applications

Uterus

Previously, it has been shown that UPK1B, which was upregulated in our canine endometrial organoids, was upregulated after an endometrial biopsy, and the protein was found in glandular-

epithelial cells (Kalma et al., 2009). Human endometrium organoids typically resemble a cystic-shaped organoid unlike the canine endometrial organoids, which contained large tubule structures (**Figure 1**) (Boretto et al., 2017; Turco et al., 2017). One study administered hormones to the culture and noticed columnar epithelial morphology with the formation of larger vacuoles (Cindrova-Davies et al., 2021). Previously, cultures of 3D uterine glands explants and stromal cells had limited viability surviving only for four days with the resemblance of spheroids beginning to form (Stadler et al., 2009). Endometrium organoids may be useful for investigating endometriosis and endometrial cancers (Turco et al., 2017), as well as studies regarding implantation (Rawlings et al., 2021). Research regarding human physiology and the function of the endometrium is difficult due to variability between individuals; however, co-culturing endometrium organoids on three-dimensional scaffolds may allow investigation into implantation studies (Cindrova-Davies et al., 2021).

Lung

Canine lung organoids contained a variety of distinct morphologies (**Figure 1**); however, due to the differences in their abundance, the expression of the least populated phenotypes was difficult to determine using bulk RNASeq. Nonetheless, phenotypic and genotypic characterization suggest that our culture does contain alveolar type 2 (AT2) cells. AT2 cells are responsible for expression of surfactant proteins in the lungs and differentiation into AT1 cells which cover more than 95% of the alveolar surface area and are crucial for gas-exchange (Barkauskas et al., 2013; Wang et al., 2018b). Lung organoid models have recently helped uncover cell pathways critical during lung repair and regeneration and identify damage-associated transient progenitors (DATPs) which represent a distinct population of AT2-lineage cells (Choi et al., 2020). Having both bronchial epithelial cells and AT2 cell types present in our lung organoids increases the number of future potential applications of the organoids. It has been shown that the lung arises from cells expressing the NKX2-1 transcription factor (Kaushik

et al., 2018), which is upregulated in our lung organoids. For example, lung organoids have previously been used in the Transwell system for studying viral uptake into cells (Zhou et al., 2018). The use of a lung organoid model derived from human pluripotent stem cells showed that AT2-like cells are susceptible to SARS-CoV-2 infection, and infection of organoids resulted in the upregulation of chemokines similar to that reported in patients with COVID-19 (Han et al., 2021). Similarly, canine lung organoids could be used for in-depth pathophysiology studies of viruses causing various canine respiratory diseases.

Pancreas

The characterization of the canine pancreas-derived organoids suggests that they primarily contain intercalated pancreatic ductular cells (**Figure 1**). In addition, we believe it is possible that small endocrine cell populations were beginning to form in the organoids (**Figure 1**). In dogs, pancreatitis is overwhelmingly the most common disease of the exocrine pancreas (Lim et al., 2014; Xenoulis, 2015), therefore, a healthy pancreatic canine organoid model could assist in studying the pathophysiology of pancreatitis in this species. Murine *in vivo* models have long been known to have limited translatability for modeling pancreatic cancer in humans (Bailey and Carlson, 2019). Canine pancreatic ductal organoids could potentially be used for disease modeling of pancreatic ductal adenocarcinoma (PDAC), which is one of the most lethal types of cancer in humans (Wiedenmann et al., 2021). Furthermore, differentiation of our canine pancreatic cultures can be attempted in the future since recently described methods successfully differentiated 2D canine pancreatic ductal cells into insulin- and glucagon-producing beta-like cells (Gao et al., 2022). Such applications could then be used for hormone production and studying drug target screening and toxicological effects on the pancreas.

Kidney

Madin-Darby canine kidney (MDCK) cells have been extensively used to study permeability- and efflux-transport of drugs developed for the human market (Ye et al., 2020). The MDCK model and other immortalized cell lines fail to display functional differentiation and cannot completely recapitulate the phenotype of the primary cell (Ashammakhi et al., 2018). Due to the rapid evolution of organoid technology, genetic editing of kidney organoids for disease modeling and the use of organ-on-a-chip technology hold much promise in drug development (Ashammakhi et al., 2018). Previously adult canine kidney epithelial stem cells were grown, but these simply gave rise to dome-forming tubular organoids (Chen et al., 2019). Here we describe the derivation of the 3D canine kidney organoids, with unique morphology mimicking the tissue of origin (**Figure 1**), which in the future, by culturing them on transwells, could be used for drug screening purposes and eventually replace the use of the MDCK system (Nishinakamura, 2019). While dogs and humans differ in some kidney influx and efflux transporters, many commonalities could allow canine kidney organoids to be used for drug development and as a tool for greater understanding of kidney toxicity in veterinary and human medicine (Martinez et al., 2021).

Urinary Bladder

Canine bladder cancer organoids were previously described and exposed to anticancer drugs to describe their potential role in research and precision medicine (Elbadawy et al., 2019). Since canine bladder cancer is a well-established model for human muscle-invasive bladder cancer (Knapp et al., 2020), canine bladder cancer organoids represent a valuable model for translational preclinical research (Minkler et al., 2021). In addition, Elbadawy et al. has recently described healthy canine bladder organoids (Elbadawy et al., 2022). This report expands the knowledge and accessibility of healthy canine bladder organoids, with those described here displaying a similar morphological phenotype to those previously described (**Figure 1**)

(Elbadawy et al., 2022). Using 3D patient-derived tumor organoids to predict the response to chemotherapeutic protocols has great potential in oncological precision medicine. Therefore, there is a need for healthy canine bladder organoids to serve as controls when attempting to identify novel immunotherapeutic strategies (Yu et al., 2021).

Liver

Canine liver-derived organoids have previously been described from both normal and *COMMD1*-deficient dogs to model copper storage disease, which is also known as Wilson's disease in humans (Nantasanti et al., 2015). Our group has recently further standardized the protocol for canine hepatic organoid culture (Gabriel et al., 2022a). Based on this characterization, our canine liver organoid culture is mainly comprised of differentiated cholangiocytes (**Figure 1**). The previous study describing canine hepatic organoids in expansion media showed that the organoids minimally expressed the mature hepatocyte (CYP3A12) marker while stably expressing the following markers: stem cell (CD133 and LGR5), cholangiocyte (KRT19 and SOX9), and early hepatocyte (FOXA1 and HNF4α) (Nantasanti et al., 2015). Future efforts could involve the development of media compositions, including growth factors that will enhance the differentiation of hepatic stem cells into mature, differentiated hepatocytes rather than cholangiocytes, which were first described in murine liver organoids (Huch et al., 2013), then first attempted in dogs (Nantasanti et al., 2015), and further refined in dogs (Kruitwagen et al., 2020). Optimization of this differentiation could open avenues to explore their usefulness for hepatic toxicity assays in addition to modeling various analogous cholangiopathies and hepatocellular diseases.

CONCLUSION

Applications of organoid technologies are rapidly expanding and now encompass protocols to develop reliable *in vitro* models of various diseases. Further differentiation or enrichment of

certain cell populations within the organoids characterized here is warranted to expand the current scope of applications for canine organoids. We report the successful isolation, culture, and characterization of three novel canine organoid lines. These novel organoid lines will enhance future use of the technology in fields including drug development, pathogen and host interactions, clinical applications, and personalized medicine applications. Furthermore, a multi-tissue comparison of six canine organoid lines derived from two genetically related individuals allowed for tissue-specific expression patterns to be reported. The antibodies optimized in this study for the canine model can be used for differentiation experiments attempting to enrich specific cell types such as differentiated hepatocytes and pancreatic beta cells. Future directions, including derivation of organoids from adult and diseased canines and further characterization utilizing single-cell RNA sequencing, will help identify unique subpopulations of cells within the organoids, further increasing the applicability of these new translational *in vitro* models.

EXPERIMENTAL PROCEDURES

Tissue collection

Dogs were used under permit (ref. IACUC-18-065), and proper Institutional Animal Care and Use Committee (IACUC) protocols were followed. For this study, two 4-week-old intact female canines were euthanized via intravenous sodium pentobarbital overdose due to unrelated reasons, and tissues were quickly harvested (donor details in **Table S2**). Biopsies were rinsed three times in 10 mL of 1X Complete Chelating Solution (1X CCS, composition and further details can be found in Gabriel et al. 2022) and transferred to 6 mL of Dulbecco's Modified Eagle Medium/Nutrient Mixture F-12 (Advanced DMEM/F12) with the addition of Pen Strep (Gabriel et al., 2022a).

Organoid isolation and cultivation

Organoid isolation and maintenance were based on a modified protocol described by Saxena et al. in 2016, which was optimized to include the standardized culture, expansion, and harvesting of canine intestinal and hepatic organoids in Gabriel et al. 2022 (Gabriel et al., 2022a; Saxena et al., 2016). Modifications to the original protocol included using both Matrigel compositions Phenol red-free (Corning ref. 356231) and Phenol red (Corning ref. 356230) and Y-27632, which was supplied by Biogems. After successful expansion in our growth media (CMGF+ R/G), both Y-27632 ROCK inhibitor and GSK3β were retracted (CMGF+) for five days to discourage the culture from stem cell expansion and allow time for potential differentiation of cell lines to occur prior to harvesting for characterization (see **Table S3** for complete media details).

RNA extractions and sequencing

After isolation, expansion, and differentiation (between 17 and 31 days), organoids were pelleted and resuspended in 100 µL of Phosphate Buffered Saline (PBS) and transferred to a cryovial. The sample tube was flushed with 900 µL of RNAlater and subsequently added to the cryovial before being stored in liquid nitrogen (-196°C). Tissue biopsies were directly placed into cryovials containing 1 mL of RNAlater and stored in liquid nitrogen. Upon thawing, tissue samples were quickly rinsed in PBS to remove excess salts from the RNAlater solution and were immediately transferred to 800 µL of Trizol and homogenized with a pestle. Organoid samples were thawed and transferred to a 15 mL tube with 2 mL of PBS, then spun at 1,200 g at 4°C for 5 min to pellet the organoids. RNAlater was removed, and 1 mL of Trizol was added to the organoids and homogenized via brief vortexing.

After homogenizing, samples were stored at room temperature for 5 minutes and then spun at 12,000 g at 4°C for 10 min to eliminate debris and polysaccharides. The supernatant was transferred to a new tube, and chloroform (0.2 mL chloroform per mL Trizol) was added.

Samples were shaken vigorously for 20 sec and stored at room temperature for 2-3 minutes before being spun at 10,000 g at 4°C for 18 minutes. The aqueous phase was transferred to a sterile 1.5 mL RNase-free tube. Then an equal volume of 100% RNA-free EtOH was slowly added and mixed before being transferred to a Qiagen RNeasy column (RNeasy Mini kit) seated in a collection tube which was spun for 30 seconds at 8,000 g. Flow-through was discarded, and the Qiagen DNase treatment protocol was followed. Next, 500 µL of buffer RPE was added and spun for 30 seconds at 8,000 g. Flow-through was again discarded, and 500 µL of buffer RPE was added and spun for 2 minutes at 8,000 g. Flow-through was discarded, and columns were spun for 1 minute at 8,000 g to remove the remaining buffer. RNA was eluted in 50 µL of RNase-free water and allowed to sit for 2 minutes before being spun for 1 minute at 8,000 g. Samples were spun again at 8,000 g, immediately analyzed on a Nanodrop, and frozen at -80°C.

Prior to library preparation, RNA samples were quantified with an Agilent 2100 Bioanalyzer (Eukaryotic Total RNA Nano). Further quantification was done by GENEWIZ using a Qubit 2.0 Fluorometer (ThermoFisher Scientific) and a 4200 Tapestation (Agilent). An ERCC RNA Spike-In Mix kit (ThermoFisher Scientific cat. 4456740) was used to normalize total RNA prior to library preparation. A NEBNext Ultra II RNA Library Prep Kit for Illumina (New England Biolabs, Ipswich, MA, USA) was used for library preparation. mRNAs were initially enriched with Oligod(T) beads and then fragmented for 15 minutes at 94°C. Next, first and second-strand cDNA was synthesized, end-repaired, and adenylated at 3'ends, and universal adapters were ligated to cDNA fragments. This was followed by index addition and library enrichment by PCR with limited cycles. Libraries were validated on the Agilent TapeStation (Agilent Technologies, Palo Alto, CA, USA) and quantified using a Qubit 2.0 Fluorometer (ThermoFisher Scientific, Waltham, MA, USA) as well as by quantitative PCR (KAPA Biosystems, Wilmington, MA, USA). The libraries were multiplexed and clustered onto two flowcells and were loaded onto an Illumina HiSeq 4000 instrument. The samples were sequenced using a 2x150bp Paired-End

(PE) configuration. The HiSeq Control Software (HCS) conducted image analysis and base calling. Raw sequence data (.bcl files) generated from Illumina HiSeq was converted into fastq files and de-multiplexed using Illumina bcl2fastq 2.20 software with one mismatch allowed for index sequence identification.

RNA sequencing

The total number of reads from tissues and organoids ranged from ~18×10^6 to 27×10^6 (**Table S4**). The average Phred quality score was 35 before quality control procedures (see *Processing, mapping, and quantification of RNASeq libraries*). Comparisons were made between organoids and their native tissues, across organoids, and across tissues, for both B816 and B818 individuals.

Processing, mapping, and quantification of RNASeq libraries

Raw sequence files were inspected in FastQC v0.11 and MultiQC v1.7 (Kim et al., 2015; Li et al., 2009) to verify their quality. Barcodes were trimmed from reads and reads with a quality score < 20 were discarded from downstream analysis cutadapt v3.5 (Martin, 2011). The data set was de-duplicated with BBDuK v38.94 (https://sourceforge.net/projects/bbmap/) with a search k-mer size of 18bp. The resulting reads were passed to SortMeRNA v2.1 (Kopylova et al., 2012) to filter out rRNA sequences based on similarity with the SILVA v111 and Rfam v11.0 databases (Gardner et al., 2009; Quast et al., 2013). After each step, reads were inspected with FastQC and MultiQC to ensure the quality of the data. Prior to the alignment of reads to a dog genome with STAR v2.5, an index was created from ROS_Cfam_1.0 (RefSeq: GCF_014441545). In average for all samples, 90.3% of the reads mapped to unique targets within the reference genome (**Table S4**). Sequences from the ERCC spike-in controls were included in this index to quantify their abundances in the samples. The resulting BAM files were passed to Subread v1.6 to obtain gene-level counts via the featureCounts algorithm.

Differential gene expression analysis

Gene counts mapped to ERCC spike-in controls by featureCounts were extracted. Then, we calculated library size scaling factors based solely on ERCC counts using edgeR v3.36 (Robinson et al., 2009) as implemented in R v4.1 (Team, 2013) and using the trimmed mean of M-values (TMM) method (Robinson and Oshlack, 2010) to normalize the ERCC counts. The scaling factors were used to normalize the gene counts and calculate log2-transformed counts per million (CPM) after adding a 0.5 as a constant to all the values.

Our goal was to detect differences in gene expression between extracted tissues and the corresponding organoids. Prior to differential gene expression analysis, exploration of the whole transcriptome was done by multidimensional scaling and looking for the overall transcriptomic similarity between samples as expected by origin (endometrium, lung, pancreas, kidney, bladder, or liver) and type (extracted or organoid). No obvious outliers were detected during this exploratory analysis. The model under testing was expr=β_1+β_2 x organoid, with type indicating if the sample was an organoid or not. Gene-wise dispersions were estimated, and outlier effects were reduced with the estimateDisp function in edgeR (using the robust=T option). Negative binomial generalized linear models (GLM) were fitted for each gene, and statistical significance for the difference in mean expression was obtained by performing Bayes quasi-likelihood F-tests (glmQLFTest function in edgeR). Visualization of the results via heatmaps and Venn diagrams were generated via the ComplexHeatmap (Gu et al., 2016) and VennDiagram (Chen and Boutros, 2011) R packages. Genes unique to each organ are listed in **Table S5** and **Table S6**.

Gene set enrichment analysis using g:Profiler

Functional enrichment analysis was performed using g:Profiler (version e106_eg53_p16_65fcd97) (Raudvere et al., 2019). The genes unique to each organ were used

and sorted based off the highest logFC values for both organoids and tissues. The *Canis lupus familiaris* (Dog) dataset from Ensembl was used and the following data sources were used: GO molecular function (GO: MF), GO cellular component (GO: CC), GO biological process (GO: BP), KEGG (biological pathways), and HP (Human phenotype ontology). All ambiguous query genes were ignored, the significance threshold used was the g:SCS threshold, and the user threshold was set to 0.05.

Paraffin embedding and immunohistochemistry

After organoids were expanded, they were then allowed to grow in CMGF+ for five days, media was removed, and 500 µL of Formalin-acetic acid-alcohol (FAA, composition in Gabriel et al. 2022) was added to each well (Gabriel et al., 2022a). After 24 hours, FAA was replaced with 70% ethanol and samples were paraffin-embedded and mounted on slides at the Iowa State University Histopathology laboratory. Tissues were fixed in paraformaldehyde and paraffin-embedded according to standard histology procedures. Tissues and organoids were stained with hematoxylin and eosin and light microscopy images were taken on a Leica Aperio GT 450 Scanner and analyzed with ImageScope (v12.4.3.5008).

Immunofluorescence

For deparaffinization, slides were placed in xylene twice for ten minutes, then transferred to 100% ethanol twice for one minute with regular agitation. After the last alcohol wash, slides were laid on tissue paper for five minutes to dry. After deparaffinization, tissues and organoids underwent Heat Induced Epitope Retrieval (HIER) with either Citrate buffer (pH 6) or a Tris/EDTA buffer (pH 9) using a HybEZ II Oven at 75°C for two hours. After two hours, the tray was taken out of the oven, and the slides were allowed to cool with the lid off for 15 minutes. Once cool, slides were rinsed in PBS twice for two minutes each, then rinsed in PBS for ten minutes. The tissues and organoids were permeabilized by incubating in 0.25% Triton in PBS

twice for ten minutes each. After being rinsed in PBS three times, tissues and organoids were blocked in Casein in PBS for one hour at room temperature. Tissues and organoids were incubated in a humidity chamber with their primary antibody overnight at 4°C at the appropriate concentration. The next day, slides were again rinsed in PBS, the secondary was added at 1:1000 in PBS for one hour at room temperature and slides were rinsed again. The slides were incubated with DAPI (Sigma, D9542-1MG) at 1:500 in PBS for twenty minutes, and washed three times for ten minutes in PBS, then switched to distilled water. Fluoroshield (Sigma, F6182-20ML) was used to mount the slides, and after drying overnight, the slides were imaged on a Stellaris confocal. Antibodies, dilutions, and antigen retrieval techniques for each tissue type can be seen in **Table S7**. Scale bars were added to immunofluorescent images using Leica LAS AF Lite (v. 2.6.0 build 7266).

AUTHOR CONTRIBUTIONS

Conceptualization, C.Z. and V.G.; Methodology, V.G. and C.Z.; Investigation, C.Z., V.G., O.E.O, H.W., D.K.S., K.D., L.S.A.M., L.B., S.H., and P.P.; Data Curation, O.E.O.; Writing – Original Draft, C.Z. and V.G.; Writing – Review & Editing, C.Z., V.G., O.E.O, H.W., D.K.S., K.D., L.S.A.M., L.B., S.H., P.P., J.P.M., K.A; Funding Acquisition, K.A. and J.P.M.; Supervision, K.A. and J.P.M.

CONFLICTS OF INTERESTS

K. Allenspach is a co-founder of LifEngine Animal Health and 3D Health Solutions. She serves as a consultant for Ceva Animal Health, Bioiberica, LifeDiagnostics, Antech Diagnostics, Deerland Probiotics, and Mars.

J.P. Mochel is a co-founder of LifEngine Animal Health and 3D Health Solutions. Dr. Mochel serves as a consultant for Ceva Animal Health, Boehringer Ingelheim, and Ethos Animal Health.

C. Zdyrski is an intern at 3D Health Solutions.

K. Dao is an employee of 3D Health Solutions.

Other authors do not have any conflict of interest to declare.

DATA AVAILABILITY

The RNASeq raw reads generated in this study are available in the Sequence Read Archive (NCBI-SRA BioProject PRJNA847879). The bioinformatic scripts are available on Github (https://github.com/chris-zdyrski/Novel_Canine_Organoids).

ACKNOWLEDGEMENTS

We would like to thank Dr. Jodi Smith for the use of her colony. We are also appreciative of Dr. Adrien Aertsens and Sichao Mao for their help with tissue collection. We thank Dr. Nicole Valenzuela for lending access to Iowa State University's computing resources. We thank Ahona Mukherjee for assisting with immunofluorescence and Dr. David Meyerholz for marker recommendations. We appreciate the timely processing of samples by the Iowa State University Pathology Department and the Iowa State University Histopathology Department.

FIGURES

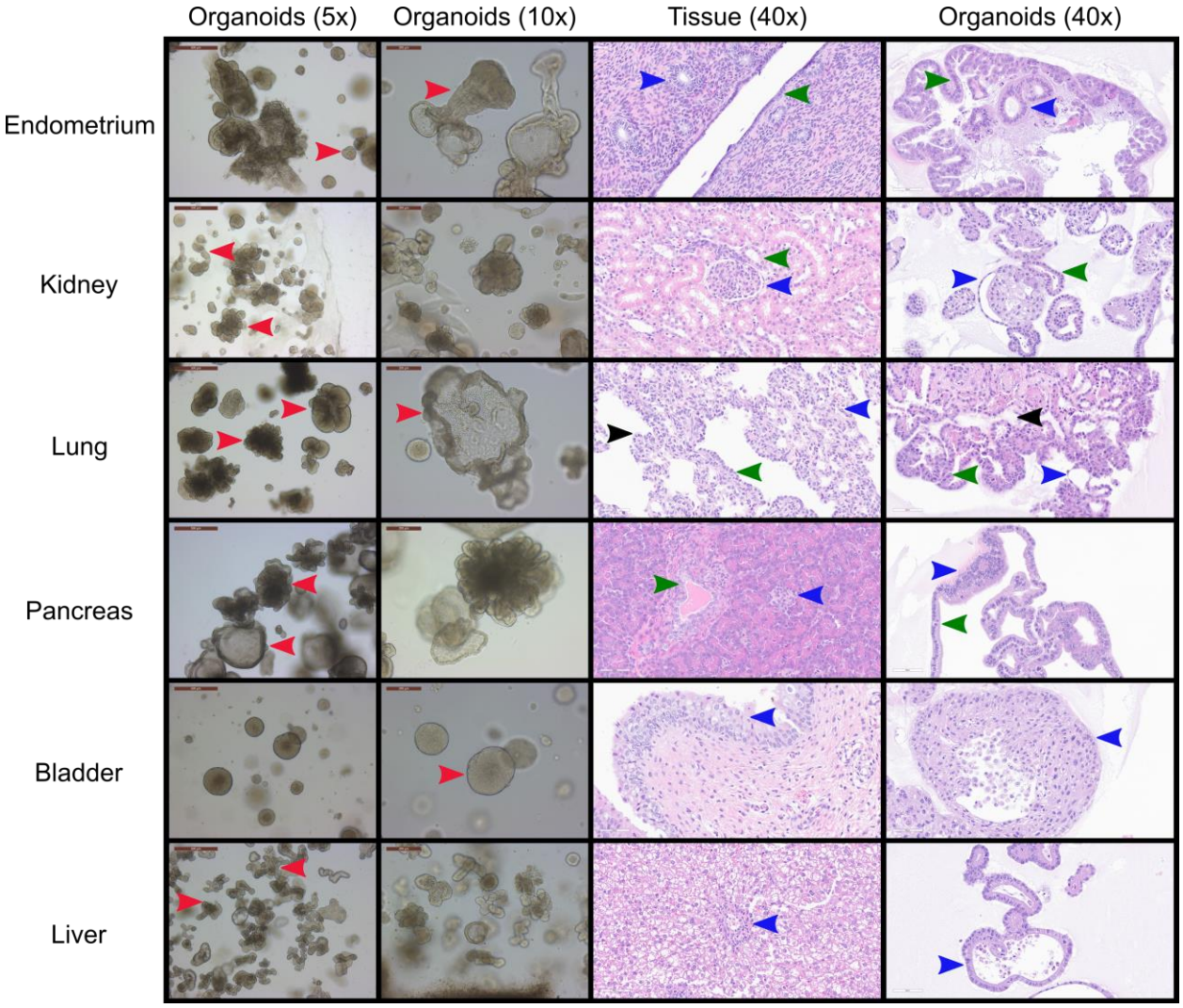

Figure 1. Morphological and histological characterization of canine organoid lines derived from a single donor.
Bright field and hematoxylin & eosin (H&E) images of six organoid cell lines derived from the uterus, lung, pancreas, kidney, bladder, and liver of canine individual B816. Red arrows indicate distinct morphologies in each organoid line while blue, green, and black arrows indicate similar histological areas of the organoids and tissues. Images of organoid cultures were captured using a Leica DMi1. Scale bars are provided at 5X (500 µm), 10X (200 µm), and 40X (60 µm) magnifications.

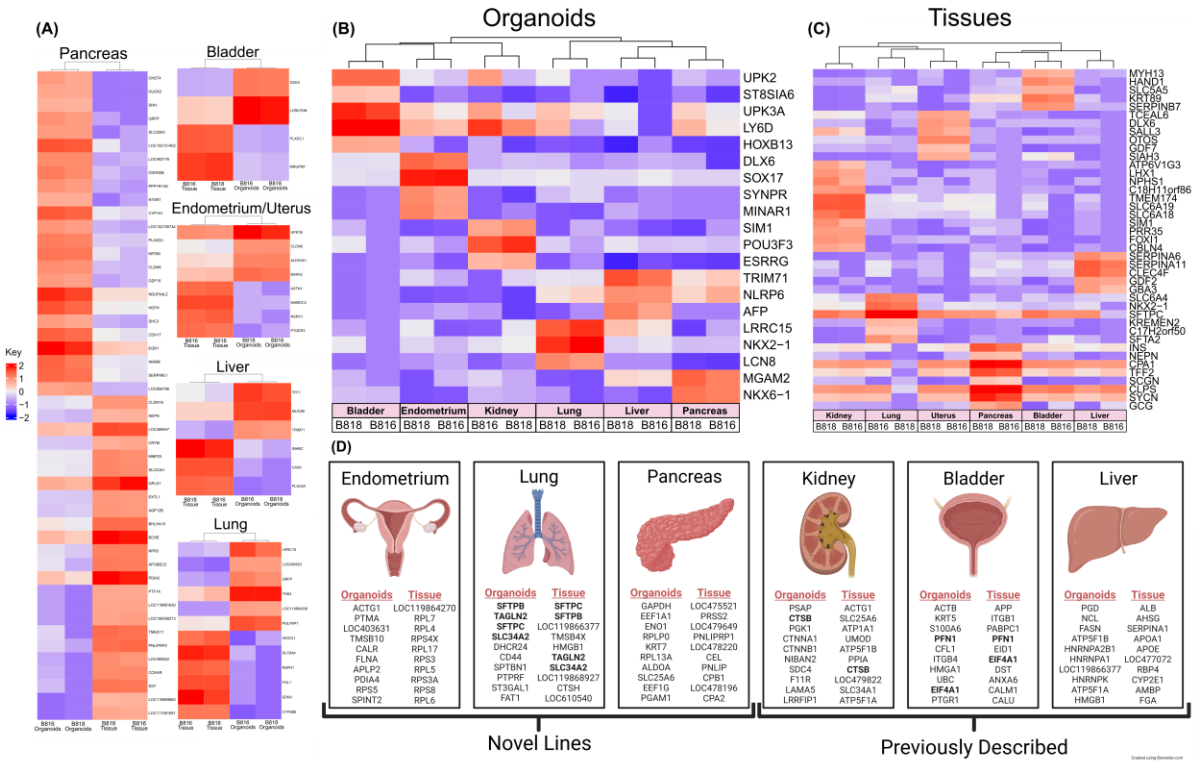

Figure 2. Expression of RNA and identification of tissue-specific markers for both organoids and tissues.

(A) RNA heatmaps of the differentially expressed (DE) genes (FWER < 0.05) between tissues and organoids of the same organs. Under the Holm–Bonferroni correction, there were no DE genes between kidney tissues and kidney-derived organoids. Tissue-specific markers were identified across the six tissues for both (B) organoids (FWER < 0.05) and (C) tissues (FWER < 0.05). Upregulated expression is red, white is neutral, and blue represents suppressed expression. (D) The ten most highly expressed tissue-specific genes from two genetically related donors for both organoids and tissues, as well as genes in common between organoids and tissues are denoted in **bold**.

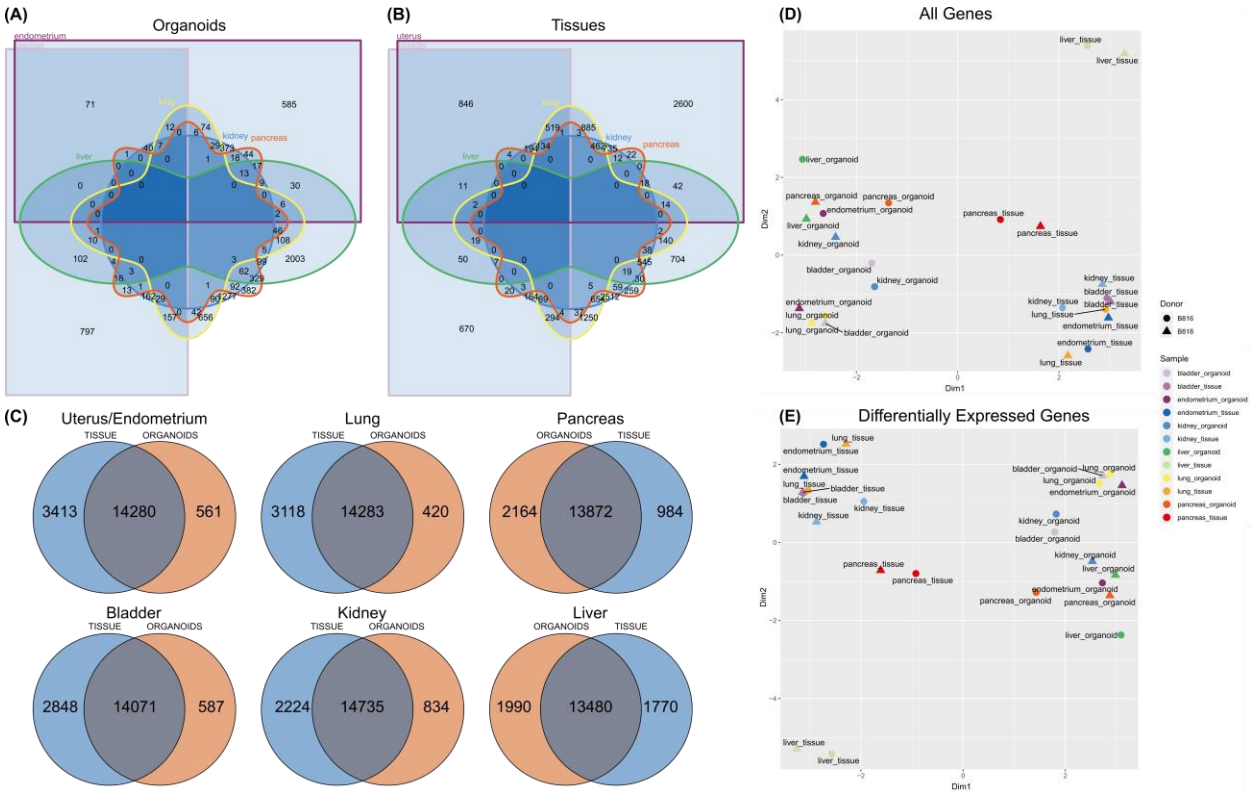

Figure 3. Comparison of mRNA expression similarity between organoids and tissue samples for each organ.

Venn diagrams of genes expressed from both donors (B816 and B818) comparing (A) organoids and (B) tissues from the same organs. (C) Venn diagrams showing the comparison of mRNA expression between organoids and tissues from each organ. Multidimensional scaling plots of mRNA expression across sample and organ types for (D) all genes and (E) differentially expressed genes. B816 is represented as a circle and B818 is denoted as a triangle. Tissue types are color coded in the legend.

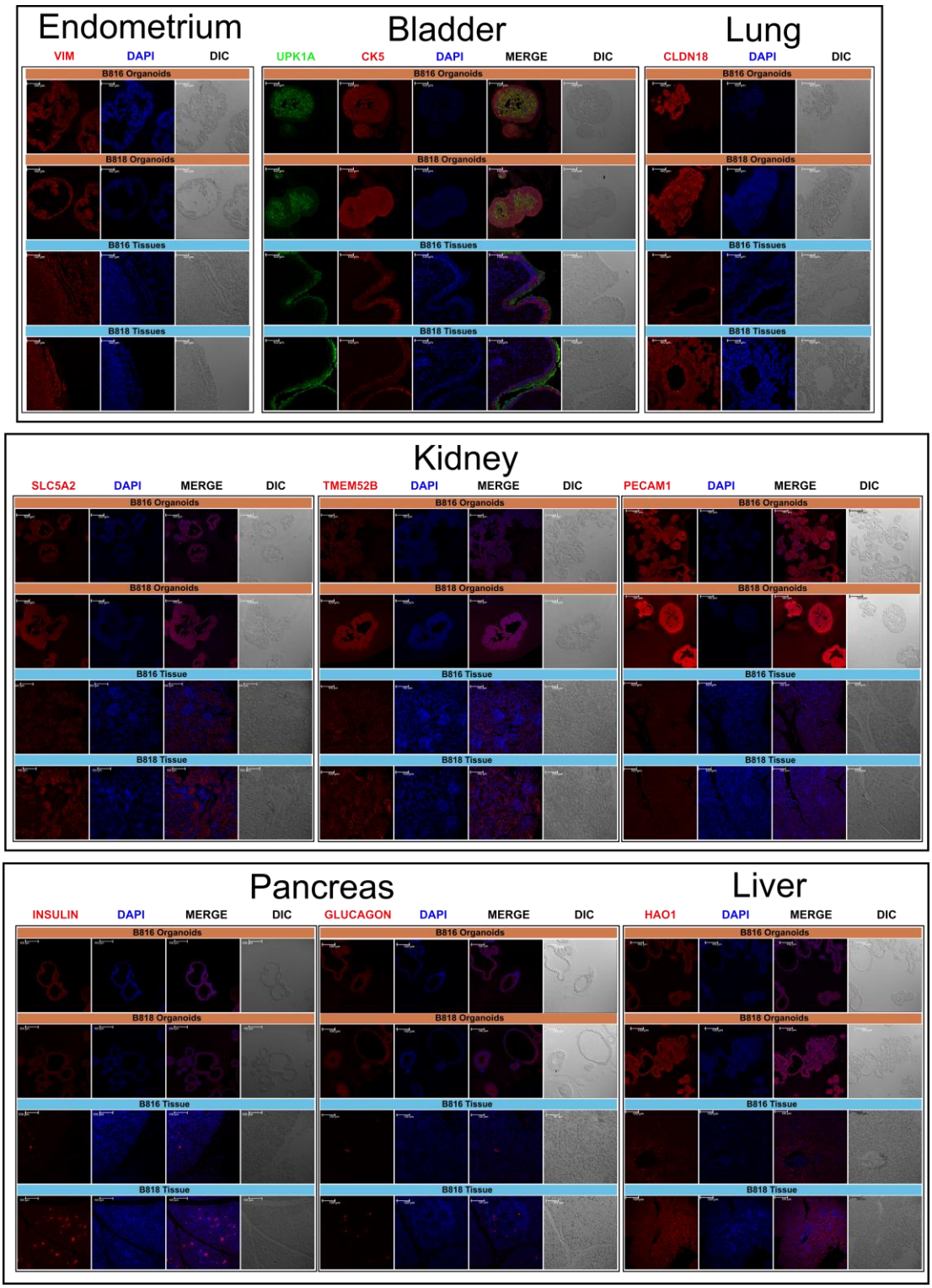

Figure 4. Protein characterization across tissues and organoids.
Immunofluorescent staining of organoids and tissues for both donors, B816 and B818. Antibodies are labeled in the channel they appear in. Images were taken at 20X magnification, scale bars are 100 µm. Immunofluorescent details are listed in **Table S7** and negative control images taken under the same conditions are shown in **Figure S1**.

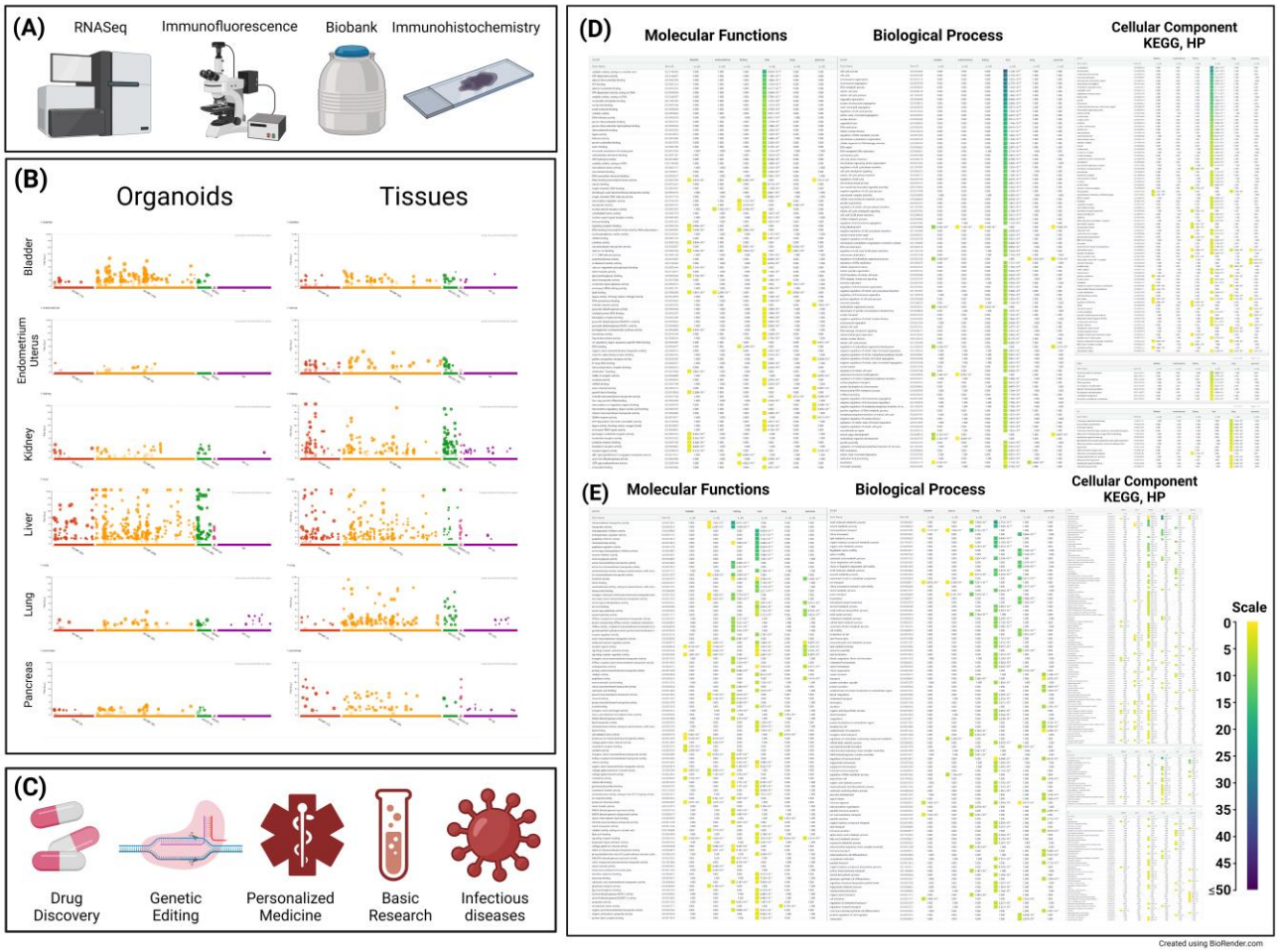

Figure 5. Characterization of novel models, g:Profiler signaling pathway enrichment analysis, and potential biomedical applications.
(A) Initial characterization and preservation methods used for the intra-donor derived canine organoid cell lines. (B) Enriched pathways of genes unique to each organ type when compared to organoids and tissues. (C) Overall biomedical applications of the canine organoid models. Functions and details of enriched pathways found across (D) organoids and (E) tissues.

LITERATURE CITED

Adin, C.A., and Gilor, C. (2017). The Diabetic Dog as a Translational Model for Human Islet Transplantation.

Ashammakhi, N., Wesseling-Perry, K., Hasan, A., Elkhammas, E., and Zhang, Y.S. (2018). Kidney-on-a-chip: untapped opportunities. Kidney International *94*, 1073–1086. https://doi.org/10.1016/j.kint.2018.06.034.

Bailey, K.L., and Carlson, M.A. (2019). Porcine models of pancreatic cancer. Frontiers in Oncology *9*. https://doi.org/10.3389/fonc.2019.00144.

Barkauskas, C.E., Cronce, M.J., Rackley, C.R., Bowie, E.J., Keene, D.R., Stripp, B.R., Randell, S.H., Noble, P.W., and Hogan, B.L.M. (2013). Type 2 alveolar cells are stem cells in adult lung. Journal of Clinical Investigation *123*, 3025–3036. https://doi.org/10.1172/JCI68782.

Bartfeld, S., and Clevers, H. (2017). Stem cell-derived organoids and their application for medical research and patient treatment. Journal of Molecular Medicine *95*, 729–738. https://doi.org/10.1007/s00109-017-1531-7.

Bellessort, B., le Cardinal, M., Bachelot, A., Narboux-Nême, N., Garagnani, P., Pirazzini, C., Barbieri, O., Mastracci, L., Jonchere, V., Duvernois-Berthet, E., et al. (2016). Dlx5 and Dlx6 control uterine adenogenesis during post-natal maturation: Possible consequences for endometriosis. Human Molecular Genetics *25*, 97–108. https://doi.org/10.1093/hmg/ddv452.

Birey, F., Andersen, J., Makinson, C.D., Islam, S., Wei, W., Huber, N., Fan, H.C., Metzler, K.R.C., Panagiotakos, G., Thom, N., et al. (2017). Assembly of functionally integrated human forebrain spheroids. Nature *545*, 54–59. https://doi.org/10.1038/nature22330.

Boretto, M., Cox, B., Noben, M., Hendriks, N., Fassbender, A., Roose, H., Amant, F., Timmerman, D., Tomassetti, C., Vanhie, A., et al. (2017). Development of organoids from mouse and human endometrium showing endometrial epithelium physiology and long-term expandability. Development (Cambridge) *144*, 1775–1786. https://doi.org/10.1242/dev.148478.

Brancato, V., Oliveira, J.M., Correlo, V.M., Reis, R.L., and Kundu, S.C. (2020). Could 3D models of cancer enhance drug screening? Biomaterials *232*. https://doi.org/10.1016/j.biomaterials.2019.119744.

Chandler, M., Cunningham, S., Lund, E.M., Khanna, C., Naramore, R., Patel, A., and Day, M.J. (2017). Obesity and Associated Comorbidities in People and Companion Animals: A One Health Perspective. Journal of Comparative Pathology *156*, 296–309. https://doi.org/10.1016/j.jcpa.2017.03.006.

Chandra, L., Borcherding, D.C., Kingsbury, D., Atherly, T., Ambrosini, Y.M., Bourgois-Mochel, A., Yuan, W., Kimber, M., Qi, Y., Wang, Q., et al. (2019). Derivation of adult canine intestinal organoids for translational research in gastroenterology. BMC Biology *17*, 1–21. https://doi.org/10.1186/s12915-019-0652-6.

Chang, H.M., Martinez, N.J., Thornton, J.E., Hagan, J.P., Nguyen, K.D., and Gregory, R.I. (2012). Trim71 cooperates with microRNAs to repress Cdkn1a expression and promote embryonic stem cell proliferation. Nature Communications *3*. https://doi.org/10.1038/ncomms1909.

Chen, H., and Boutros, P.C. (2011). VennDiagram: A package for the generation of highly-customizable Venn and Euler diagrams in R. BMC Bioinformatics *12*. https://doi.org/10.1186/1471-2105-12-35.

Chen, T.C., Neupane, M., Chien, S.J., Chuang, F.R., Crawford, R.B., Kaminski, N.E., and Chang, C.C. (2019). Characterization of Adult Canine Kidney Epithelial Stem Cells That Give Rise to Dome-Forming Tubular Cells. Stem Cells and Development *28*, 1424–1433. https://doi.org/10.1089/scd.2019.0049.

Choi, J., Park, J.E., Tsagkogeorga, G., Yanagita, M., Koo, B.K., Han, N., and Lee, J.H. (2020). Inflammatory Signals Induce AT2 Cell-Derived Damage-Associated Transient Progenitors that Mediate Alveolar Regeneration. Cell Stem Cell *27*, 366-382.e7. https://doi.org/10.1016/j.stem.2020.06.020.

Cindrova-Davies, T., Zhao, X., Elder, K., Jones, C.J.P., Moffett, A., Burton, G.J., and Turco, M.Y. (2021). Menstrual flow as a non-invasive source of endometrial organoids. Communications Biology *4*. https://doi.org/10.1038/s42003-021-02194-y.

DiMasi, J.A., Grabowski, H.G., and Hansen, R.W. (2016). Innovation in the pharmaceutical industry: New estimates of R&D costs. Journal of Health Economics *47*, 20–33. https://doi.org/10.1016/j.jhealeco.2016.01.012.

Dongeun, H., D, M.B., Akiko, M., Martín, M.-Z., Yuan, H.H., and E, I.D. (2010). Reconstituting Organ-Level Lung Functions on a Chip. Science (1979) *328*, 1662–1668. https://doi.org/10.1126/science.1188302.

Dost, A.F.M., Moye, A.L., Vedaie, M., Tran, L.M., Fung, E., Heinze, D., Villacorta-Martin, C., Huang, J., Hekman, R., Kwan, J.H., et al. (2020). Organoids Model Transcriptional Hallmarks of Oncogenic KRAS Activation in Lung Epithelial Progenitor Cells. Cell Stem Cell *27*, 663-678.e8. https://doi.org/10.1016/j.stem.2020.07.022.

Elbadawy, M., Usui, T., Mori, T., Tsunedomi, R., Hazama, S., Nabeta, R., Uchide, T., Fukushima, R., Yoshida, T., Shibutani, M., et al. (2019). Establishment of a novel experimental model for muscle-invasive bladder cancer using a dog bladder cancer organoid culture. Cancer Science *110*, 2806–2821. https://doi.org/10.1111/cas.14118.

Elbadawy, M., Fujisaka, K., Yamamoto, H., Tsunedomi, R., Nagano, H., Ayame, H., Ishihara, Y., Mori, T., Azakami, D., Uchide, T., et al. (2022). Establishment of an experimental model of normal dog bladder organoid using a three-dimensional culture method. Biomedicine & Pharmacotherapy *151*, 113105. https://doi.org/10.1016/j.biopha.2022.113105.

Gabriel, V., Zdyrski, C., Sahoo, D.K., Dao, K., Bourgois-Mochel, A., Kopper, J., Zeng, X.-L., Estes, M.K., Mochel, J.P., and Allenspach, K. (2022a). Standardization and Maintenance of 3D Canine Hepatic and Intestinal Organoid Cultures for Use in Biomedical Research. Journal of Visualized Experiments 1–28. https://doi.org/10.3791/63515.

Gabriel, V., Zdyrski, C., Sahoo, D.K., Dao, K., Bourgois-Mochel, A., Atherly, T., Martinez, M.N., Volpe, D.A., Kopper, J., Allenspach, K., et al. (2022b). Canine Intestinal Organoids in a Dual-Chamber Permeable Support System. Journal of Visualized Experiments https://doi.org/10.3791/63612.

Gao, Y., Guan, W., and Bai, C. (2022). Pancreatic Duct Cells Isolated From Canines Differentiate Into Beta-Like Pancreatic Islet Cells. Frontiers in Veterinary Science *8*. https://doi.org/10.3389/fvets.2021.771196.

Gardner, P.P., Daub, J., Tate, J.G., Nawrocki, E.P., Kolbe, D.L., Lindgreen, S., Wilkinson, A.C., Finn, R.D., Griffiths-Jones, S., Eddy, S.R., et al. (2009). Rfam: Updates to the RNA families database. Nucleic Acids Research *37*. https://doi.org/10.1093/nar/gkn766.

Gordon, I., Paoloni, M., Mazcko, C., and Khanna, C. (2009). The comparative oncology trials consortium: Using spontaneously occurring cancers in dogs to inform the cancer drug development pathway. PLoS Medicine *6*. https://doi.org/10.1371/journal.pmed.1000161.

Gu, Z., Eils, R., and Schlesner, M. (2016). Complex heatmaps reveal patterns and correlations in multidimensional genomic data. Bioinformatics *32*, 2847–2849. https://doi.org/10.1093/bioinformatics/btw313.

Han, Y., Duan, X., Yang, L., Nilsson-Payant, B.E., Wang, P., Duan, F., Tang, X., Yaron, T.M., Zhang, T., Uhl, S., et al. (2021). Identification of SARS-CoV-2 inhibitors using lung and colonic organoids. Nature *589*, 270–275. https://doi.org/10.1038/s41586-020-2901-9.

Hasiwa, N. (2011). Critical evaluation of the use of dogs in biomedical research and testing in Europe. ALTEX *28*, 326–340. https://doi.org/10.14573/altex.2011.4.326.

Hayashi, Y., Yamaguchi, J., Kokuryo, T., Ebata, T., Yokoyama, Y., and Nagino, M. (2018). Loss of trefoil factor 1 inhibits biliary regeneration but accelerates the hepatic differentiation of progenitor cells in mice. Biochemical and Biophysical Research Communications *506*, 12–19. https://doi.org/10.1016/j.bbrc.2018.10.023.

Hickman, J.A., Graeser, R., de Hoogt, R., Vidic, S., Brito, C., Gutekunst, M., van der Kuip, H., and Imi Predect consortium (2014). Three-dimensional models of cancer for pharmacology and cancer cell biology: Capturing tumor complexity in vitro/ex vivo. Biotechnology Journal *9*, 1115–1128. https://doi.org/10.1002/biot.201300492.

Huch, M., and Koo, B.K. (2015). Modeling mouse and human development using organoid cultures. Development (Cambridge) *142*, 3113–3125. https://doi.org/10.1242/dev.118570.

Huch, M., Dorrell, C., Boj, S.F., van Es, J.H., Li, V.S.W., van de Wetering, M., Sato, T., Hamer, K., Sasaki, N., Finegold, M.J., et al. (2013). In vitro expansion of single Lgr5 + liver stem cells induced by Wnt-driven regeneration. Nature *494*, 247–250. https://doi.org/10.1038/nature11826.

Hynds, R.E., and Giangreco, A. (2013). Concise review: The relevance of human stem cell-derived organoid models for epithelial translational medicine. Stem Cells *31*, 417–422. https://doi.org/10.1002/stem.1290.

Jones, R.C., Karkanias, J., Krasnow, M.A., Pisco, A.O., Quake, S.R., Salzman, J., Yosef, N., Bulthaup, B., Brown, P., Harper, W., et al. (2022). The Tabula Sapiens: A multiple-organ, single-cell transcriptomic atlas of humans. Science (1979) *376*. https://doi.org/10.1126/science.abl4896.

Kalma, Y., Granot, I., Gnainsky, Y., Or, Y., Czernobilsky, B., Dekel, N., and Barash, A. (2009). Endometrial biopsy-induced gene modulation: first evidence for the expression of bladder-transmembranal uroplakin Ib in human endometrium. Fertility and Sterility *91*. https://doi.org/10.1016/j.fertnstert.2008.01.043.

Kampf, C., Mardinoglu, A., Fagerberg, L., Hallström, B.M., Edlund, K., Lundberg, E., Pontén, F., Nielsen, J., and Uhlen, M. (2014). The human liver-specific proteome defined by transcriptomics and antibody-based profiling. FASEB Journal *28*, 2901–2914. https://doi.org/10.1096/fj.14-250555.

Kaushik, G., Ponnusamy, M.P., and Batra, S.K. (2018). Concise Review: Current Status of Three-Dimensional Organoids as Preclinical Models. Stem Cells *36*, 1329–1340. https://doi.org/10.1002/stem.2852.

Kim, D., Langmead, B., and Salzberg, S.L. (2015). HISAT: A fast spliced aligner with low memory requirements. Nature Methods *12*, 357–360. https://doi.org/10.1038/nmeth.3317.

Kim, E., Choi, S., Kang, B., Kong, J.H., Kim, Y., Yoon, W.H., Lee, H.R., Kim, S.E., Kim, H.M., Lee, H.S., et al. (2020a). Creation of bladder assembloids mimicking tissue regeneration and cancer. Nature *588*, 664–669. https://doi.org/10.1038/s41586-020-3034-x.

Kim, J., Koo, B.K., and Knoblich, J.A. (2020b). Human organoids: model systems for human biology and medicine. Nature Reviews Molecular Cell Biology *21*, 571–584. https://doi.org/10.1038/s41580-020-0259-3.

Kinnear, S., Salamonsen, L.A., Francois, M., Harley, V., and Evans, J. (2019). Uterine SOX17: a key player in human endometrial receptivity and embryo implantation. Scientific Reports *9*. https://doi.org/10.1038/s41598-019-51751-3.

Knapp, D.W., Dhawan, D., Ramos-Vara, J.A., Ratliff, T.L., Cresswell, G.M., Utturkar, S., Sommer, B.C., Fulkerson, C.M., and Hahn, N.M. (2020). Naturally-Occurring Invasive Urothelial Carcinoma in Dogs, a Unique Model to Drive Advances in Managing Muscle Invasive Bladder Cancer in Humans. Frontiers in Oncology *9*. https://doi.org/10.3389/fonc.2019.01493.

Kopylova, E., Noé, L., and Touzet, H. (2012). SortMeRNA: Fast and accurate filtering of ribosomal RNAs in metatranscriptomic data. Bioinformatics *28*, 3211–3217. https://doi.org/10.1093/bioinformatics/bts611.

Kruitwagen, H.S., Oosterhoff, L.A., van Wolferen, M.E., Chen, C., Nantasanti Assawarachan, S., Schneeberger, K., Kummeling, A., van Straten, G., Akkerdaas, I.C., Vinke, C.R., et al. (2020). Long-Term Survival of Transplanted Autologous Canine Liver Organoids in a COMMD1-Deficient Dog Model of Metabolic Liver Disease. Cells *9*. https://doi.org/10.3390/cells9020410.

Lehmann, R., Lee, C.M., Shugart, E.C., Benedetti, M., Charo, R.A., Gartner, Z., Hogan, B., Knoblich, J., Nelson, C.M., and Wilson, K.M. (2019). Human organoids: A new dimension in cell biology. Molecular Biology of the Cell *30*, 1129–1137. https://doi.org/10.1091/mbc.E19-03-0135.

Li, H., Handsaker, B., Wysoker, A., Fennell, T., Ruan, J., Homer, N., Marth, G., Abecasis, G., and Durbin, R. (2009). The Sequence Alignment/Map format and SAMtools. Bioinformatics *25*, 2078–2079. https://doi.org/10.1093/bioinformatics/btp352.

Lin, C., Yin, Y., Stemler, K., Humphrey, P., Kibel, A.S., Mysorekar, I.U., and Ma, L. (2013). Constitutive β-catenin activation induces male-specific tumorigenesis in the bladder urothelium. Cancer Research *73*, 5914–5925. https://doi.org/10.1158/0008-5472.CAN-12-4198.

Lu, J., Zhao, M., Wu, C., Chu, C., Zhang, C.Z., and Cao, Y. (2022). Comparison of RNAscope and immunohistochemistry for evaluation of the UPK2 status in urothelial carcinoma tissues. Diagnostic Pathology *17*. https://doi.org/10.1186/s13000-022-01191-x.

MacParland, S.A., Liu, J.C., Ma, X.Z., Innes, B.T., Bartczak, A.M., Gage, B.K., Manuel, J., Khuu, N., Echeverri, J., Linares, I., et al. (2018). Single cell RNA sequencing of human liver reveals distinct intrahepatic macrophage populations. Nature Communications *9*. https://doi.org/10.1038/s41467-018-06318-7.

Martin, M. (2011). Cutadapt removes adapter sequences from high-throughput sequencing reads. EMBnet J *17*, 10. https://doi.org/10.14806/ej.17.1.200.

Martinez, M.N., Mochel, J.P., Neuhoff, S., and Pade, D. (2021). Comparison of Canine and Human Physiological Factors: Understanding Interspecies Differences that Impact Drug Pharmacokinetics. AAPS Journal *23*. https://doi.org/10.1208/s12248-021-00590-0.

Minkler, S., Lucien, F., Kimber, M.J., Sahoo, D.K., Bourgois-Mochel, A., Musser, M., Johannes, C., Frank, I., Cheville, J., Allenspach, K., et al. (2021). Emerging roles of urine-derived components for the management of bladder cancer: One man’s trash is another man’s treasure. Cancers (Basel) *13*, 1–13. https://doi.org/10.3390/cancers13030422.

Mochel, J.P., Jergens, A.E., Kingsbury, D., Kim, H.J., Martín, M.G., and Allenspach, K. (2018). Intestinal Stem Cells to Advance Drug Development, Precision, and Regenerative Medicine: A Paradigm Shift in Translational Research. The AAPS Journal *20*, 17. https://doi.org/10.1208/s12248-017-0178-1.

Mohammadi, S., Morell-Perez, C., Wright, C.W., Wyche, T.P., White, C.H., Sana, T.R., and Lieberman, L.A. (2021). Assessing donor-to-donor variability in human intestinal organoid cultures. Stem Cell Reports *16*, 2364–2378. https://doi.org/https://doi.org/10.1016/j.stemcr.2021.07.016.

Mollaki, V. (2021). Ethical challenges in organoid use. BioTech *10*. https://doi.org/10.3390/biotech10030012.

Mullenders, J., de Jongh, E., Brousali, A., Roosen, M., Blom, J.P.A., Begthel, H., Korving, J., Jonges, T., Kranenburg, O., Meijer, R., et al. (2019). Mouse and human urothelial cancer organoids: A tool for bladder cancer research. Proc Natl Acad Sci U S A *116*, 4567–4574. https://doi.org/10.1073/pnas.1803595116.

Munsie, M., Hyun, I., and Sugarman, J. (2017). Ethical issues in human organoid and gastruloid research. Development (Cambridge) *144*, 942–945. https://doi.org/10.1242/dev.140111.

Nantasanti, S., Spee, B., Kruitwagen, H.S., Chen, C., Geijsen, N., Oosterhoff, L.A., van Wolferen, M.E., Pelaez, N., Fieten, H., Wubbolts, R.W., et al. (2015). Disease modeling and gene therapy of copper storage disease in canine hepatic organoids. Stem Cell Reports *5*, 895–907. https://doi.org/10.1016/j.stemcr.2015.09.002.

Nishinakamura, R. (2019). Human kidney organoids: progress and remaining challenges. Nature Reviews Nephrology *15*, 613–624. https://doi.org/10.1038/s41581-019-0176-x.

van Norman, G.A. (2016). Drugs, Devices, and the FDA: Part 1: An Overview of Approval Processes for Drugs. JACC: Basic to Translational Science *1*, 170–179. https://doi.org/10.1016/j.jacbts.2016.03.002.

Ozawa, M., Inoue, M., Uchida, K., Chambers, J.K., Takeuch, Y., and Nakayama, H. (2019). Physical signs of canine cognitive dysfunction. Journal of Veterinary Medical Science *81*, 1829–1834. https://doi.org/10.1292/jvms.19-0458.

Perlman, R.L. (2016). Mouse Models of Human Disease: An Evolutionary Perspective. Evolution, Medicine, and Public Health eow014. https://doi.org/10.1093/emph/eow014.

Quast, C., Pruesse, E., Yilmaz, P., Gerken, J., Schweer, T., Yarza, P., Peplies, J., and Glöckner, F.O. (2013). The SILVA ribosomal RNA gene database project: Improved data processing and web-based tools. Nucleic Acids Research *41*. https://doi.org/10.1093/nar/gks1219.

Raudvere, U., Kolberg, L., Kuzmin, I., Arak, T., Adler, P., Peterson, H., and Vilo, J. (2019). G:Profiler: A web server for functional enrichment analysis and conversions of gene lists (2019 update). Nucleic Acids Research *47*, W191–W198. https://doi.org/10.1093/nar/gkz369.

Rawlings, T.M., Makwana, K., Tryfonos, M., and Lucas, E.S. (2021). Organoids to model the endometrium: implantation and beyond. Reproduction and Fertility *2*, R85–R101. https://doi.org/10.1530/raf-21-0023.

Robinson, M.D., and Oshlack, A. (2010). A scaling normalization method for differential expression analysis of RNA-seq data. Genome Biology *11*. https://doi.org/10.1186/gb-2010-11-3-r25.

Robinson, M.D., McCarthy, D.J., and Smyth, G.K. (2009). edgeR: A Bioconductor package for differential expression analysis of digital gene expression data. Bioinformatics *26*, 139–140. https://doi.org/10.1093/bioinformatics/btp616.

Russell, W.M.S., and Burch, R.L. (1959). The principles of humane experimental technique (Methuen).

Sampaziotis, F., Muraro, D., Tysoe, O.C., Sawiak, S., Beach, T.E., Godfrey, E.M., Upponi, S.S., Brevini, T., Wesley, B.T., Garcia-Bernardo, J., et al. (2021a). Cholangiocyte organoids can

repair bile ducts after transplantation in the human liver. Science (1979) *371*, 839–846. https://doi.org/10.1126/science.aaz6964.

Sampaziotis, F., Muraro, D., Tysoe, O.C., Sawiak, S., Beach, T.E., Godfrey, E.M., Upponi, S.S., Brevini, T., Wesley, B.T., Garcia-Bernardo, J., et al. (2021b). Cholangiocyte organoids can repair bile ducts after transplantation in the human liver. Science (1979) *371*, 839–846. https://doi.org/10.1126/science.aaz6964.

Saxena, K., Blutt, S.E., Ettayebi, K., Zeng, X.-L., Broughman, J.R., Crawford, S.E., Karandikar, U.C., Sastri, N.P., Conner, M.E., Opekun, A.R., et al. (2016). Human Intestinal Enteroids: a New Model To Study Human Rotavirus Infection, Host Restriction, and Pathophysiology. Journal of Virology *90*, 43–56. https://doi.org/10.1128/jvi.01930-15.

Schaefer, K., Rensing, S., Hillen, H., Burkhardt, J.E., and Germann, P.G. (2016). Is Science the only Driver in Species Selection? An Internal Study to Evaluate Compound Requirements in the Minipig Compared to the Dog in Preclinical Studies. Toxicologic Pathology *44*, 474–479. https://doi.org/10.1177/0192623315624572.

Schneider, B., Balbas-Martinez, V., Jergens, A.E., Troconiz, I.F., Allenspach, K., and Mochel, J.P. (2018). Model-based reverse translation between veterinary and human medicine: The one health initiative. CPT: Pharmacometrics and Systems Pharmacology *7*, 65–68. https://doi.org/10.1002/psp4.12262.

Shalev, M. (2006). New FDA recommendations to speed drug development. Lab Animal *35*, 13. https://doi.org/10.1038/laban0306-13a.

Silva, K.A.S., and Emter, C.A. (2020). Large Animal Models of Heart Failure: A Translational Bridge to Clinical Success. JACC: Basic to Translational Science *5*, 840–856. https://doi.org/10.1016/j.jacbts.2020.04.011.

Stadler, K., Handler, J., Schoenkypl, S., and Walter, I. (2009). A three-dimensional culture model of canine uterine glands. In Vitro Cellular and Developmental Biology - Animal *45*, 35–43. https://doi.org/10.1007/s11626-008-9127-8.

Subramanian, A., Sidhom, E.H., Emani, M., Vernon, K., Sahakian, N., Zhou, Y., Kost-Alimova, M., Slyper, M., Waldman, J., Dionne, D., et al. (2019). Single cell census of human kidney organoids shows reproducibility and diminished off-target cells after transplantation. Nature Communications *10*. https://doi.org/10.1038/s41467-019-13382-0.

Team, R.C. (2013). R: A language and environment for statistical computing.

Tortorella, I., Argentati, C., Emiliani, C., Martino, S., and Morena, F. (2022). The role of physical cues in the development of stem cell-derived organoids. European Biophysics Journal *51*, 105–117. https://doi.org/10.1007/s00249-021-01551-3.

Turco, M.Y., Gardner, L., Hughes, J., Cindrova-Davies, T., Gomez, M.J., Farrell, L., Hollinshead, M., Marsh, S.G.E., Brosens, J.J., Critchley, H.O., et al. (2017). Long-term, hormone-responsive organoid cultures of human endometrium in a chemically defined medium. Nature Cell Biology *19*, 568–577. https://doi.org/10.1038/ncb3516.

Usui, T., Sakurai, M., Nishikawa, S., Umata, K., Nemoto, Y., Haraguchi, T., Itamoto, K., Mizuno, T., Noguchi, S., Mori, T., et al. (2017). Establishment of a dog primary prostate cancer organoid using the urine cancer stem cells. Cancer Science *108*, 2383–2392. https://doi.org/10.1111/cas.13418.

Wang, J., Wang, T., Sun, Y., Feng, Y., Kisseberth, W.C., Henry, C.J., Mok, I., Lana, S.E., Dobbin, K., Northrup, N., et al. (2018a). Proliferative and invasive colorectal tumors in pet dogs provide unique insights into human colorectal cancer. Cancers (Basel) *10*. https://doi.org/10.3390/cancers10090330.

Wang, Y., Tang, Z., Huang, H., Li, J., Wang, Z., Yu, Y., Zhang, C., Li, J., Dai, H., Wang, F., et al. (2018b). Pulmonary alveolar type I cell population consists of two distinct subtypes that differ in cell fate. Proc Natl Acad Sci U S A *115*, 2407–2412. https://doi.org/10.1073/pnas.1719474115.

Wiedenmann, S., Breunig, M., Merkle, J., von Toerne, C., Georgiev, T., Moussus, M., Schulte, L., Seufferlein, T., Sterr, M., Lickert, H., et al. (2021). Single-cell-resolved differentiation of

human induced pluripotent stem cells into pancreatic duct-like organoids on a microwell chip. Nature Biomedical Engineering *5*, 897–913. https://doi.org/10.1038/s41551-021-00757-2.

Ye, D., Harder, A., Fang, Z., Weinheimer, M., Laplanche, L., and Mezler, M. (2020). Characterization and Validation of Canine P-Glycoprotein-Deficient MDCK II Cell Lines for Efflux Substrate Screening. Pharmaceutical Research *37*. https://doi.org/10.1007/s11095-020-02895-9.

Yu, L., Li, Z., Mei, H., Li, W., Chen, D., Liu, L., Zhang, Z., Sun, Y., Song, F., Chen, W., et al. (2021). Patient-derived organoids of bladder cancer recapitulate antigen expression profiles and serve as a personal evaluation model for CAR-T cells in vitro. Clinical and Translational Immunology *10*. https://doi.org/10.1002/cti2.1248.

Zhou, J., Li, C., Sachs, N., Chiu, M.C., Wong, B.H.-Y., Chu, H., Poon, V.K.-M., Wang, D., Zhao, X., Wen, L., et al. (2018). Differentiated human airway organoids to assess infectivity of emerging influenza virus. Proceedings of the National Academy of Sciences *115*, 6822–6827. https://doi.org/10.1073/pnas.1806308115.